Structure study of ^{42}Ca by $\alpha+^{38}$Ar cluster model: Coexistence of alpha-particle clustering and shell structure

Toshimi Sakuda
Department of Physics, Miyazaki University, Miyazaki 889-21, Japan

Shigeo Ohkubo
Department of Applied Science, Kochi Women's University, Kochi 780, Japan
(Received 21 September 1994)

The structure of ^{42}Ca is investigated by the $\alpha+^{38}$Ar orthogonality condition model. The energy spectra, α-spectroscopic factors, $E2$ transitions, and charge form factors are analyzed. On the whole, the calculated properties are in very good agreement with the experimental data. The levels are classified into the cluster and shell-model states through the analysis of the wave functions. It is emphasized that the coexistence and interplay of cluster and shell-model states are essential to the understanding of the properties of ^{42}Ca.

PACS number(s): 21.60.Gx, 27.40.+z

I. INTRODUCTION

Recently much attention has been devoted to the cluster structure in fp-shell nuclei [1–8] to extend the α-cluster structure study to nuclei heavier than the sd shell. It is quite important to verify the usefulness of an α-cluster model description in the heavier mass region. More recently, in the ^{40}Ca and ^{44}Ti nuclei parity-doublet α-cluster bands have been convincingly identified by the α-transfer experiments [9–12]. Furthermore, we have applied the α-cluster model to the ^{40}Ca nucleus [13]. This work shows that the α-cluster model is successful in accounting for the energy spectra, $E2$ transitions, and α-spectroscopic factors and gives a valuable insight into the structure of ^{40}Ca. This encourages us to explore the validity of the α-cluster model for more complicated nuclei in the fp-shell region. Since the beginning of the fp shell is analogous to the beginning of the sd shell, it seems worthwhile to make a systematic α-cluster model study of the $40 \leq A \leq 44$ nuclei.

The nucleus ^{42}Ca is well suited for this purpose. There have been many studies on ^{42}Ca [4,14–20]. There exist $4p$-$2h$ (four-particle–two-hole) core-excited candidates which cannot be described in terms of a simple shell model. The measured $E2$ transitions of the states show strong enhancement comparable to those of α-cluster bands in ^{40}Ca and ^{44}Ti. It is attractive to assign these states to the α-cluster band. It is also well known that the ground state band is mainly $(fp)^2$ shell-model states in character. The simplest and clearest example of coexistence of spherical shell-model and α-cluster states occurs for the two-nucleon+core system. The nucleus ^{42}Ca is just such a case and is analogous to the nucleus ^{18}O in the sd shell. Therefore, it is very interesting to investigate the coexistence and interplay of cluster and shell-model states in ^{42}Ca.

In this paper we will apply the microscopic $\alpha+^{38}$Ar orthogonality condition model (OCM) to ^{42}Ca, which is essentially the same approach as ^{40}Ca in Ref. [13]. The OCM has the advantage of describing the cluster and the important shell-model states in a unified way. We analyze the energy spectra, α-spectroscopic factors, $E2$ transitions, and charge form factors from the viewpoint of coexistence of α-cluster structure and shell-model structure.

II. ORTHOGONALITY CONDITION MODEL FOR THE $\alpha+^{38}$Ar SYSTEM

The model space which is described by the $\alpha+^{38}$Ar-cluster model is spanned by the wave functions

$$\Psi_J = \frac{\mathcal{A}}{\sqrt{\binom{42}{4}}} \{\phi(\alpha)\ [\ \phi_I(^{38}\mathrm{Ar})\ Y_l(\hat{\mathbf{r}})\ ]_J\ R_{Nl}(r)\}\ , \tag{1}$$

where $R_{Nl}(r)$ is a radial harmonic oscillator wave function with N oscillator quanta and $\mathcal{A}$ is the antisymmetrizer between α and ^{38}Ar. The angular momenta of ^{38}Ar and the relative motion, I and l, are coupled to the total angular momentum J. The antisymmetrized internal wave functions $\phi(\alpha)$ and $\phi_I(^{38}\mathrm{Ar})$ are assumed to be shell-model $(0s)^4$ and $(sd)^{-2}(\lambda\mu) = (04)$ configurations, respectively, with an oscillator parameter a=0.2815 fm^{-2}. The model space is generated as a direct product of the relative wave functions and the internal ones: $(N0)\times(04)$. We further classify the model space by SU(3) symmetry. Table I lists the SU(3) label $(\lambda\mu)$ for the Pauli-allowed states. The states with $N < 10$ are not allowed due to the Pauli principle. We can see that the present model space contains many important shell-model states such as the $2p$ state (6,0), the $3p$-$1h$ state (9,2), and the $4p$-$2h$ state (12,4). The configurations with

TABLE I. SU(3) classification of the allowed states of the $\alpha+^{38}$Ar system.

N	(λ,μ)				
10	(6,0)				
11	(9,2)	(8,1)	(7,0)		
12	(12,4)	(11,3)	(10,2)	(9,1)	(8,0)
13	(13,4)	(12,3)	(11,2)	(10,1)	(9,0)
⋮	⋮				
N	$(N,4)$	$(N-1,3)$	$(N-2,2)$	$(N-3,1)$	$(N-4,0)$

a larger value of N have a capacity for representing the cluster states. The inclusion of these important states enables the model to describe the coexistence of the cluster states and shell-model states in a unified way. In the present calculations, we make a truncation of the model space: the total oscillator quanta $N = 10$–30 and the relative angular momentum $l = 0$–16, which can guarantee energy convergence of the low-lying states of ^{42}Ca.

The Hamiltonian of the system is written as

$$H = H(\alpha) + H(^{38}\mathrm{Ar}) + T_{\alpha\text{-Ar}} + V_{\alpha\text{-Ar}} , \qquad (2)$$

where $H(\alpha)$ and $H(^{38}\mathrm{Ar})$ are the internal Hamiltonians for α and ^{38}Ar and $T_{\alpha\text{-Ar}}$ is the kinetic energy operator for the relative motion. The excitation energies of the 2^+ and 4^+ states of ^{38}Ar are taken from the observed spectrum as 2.17 MeV and 5.35 MeV, respectively. The intercluster potential $V_{\alpha\text{-Ar}}$ is taken to be a folding potential after the one used in Ref. [13], namely,

$$V_{\alpha\text{-Ar}} = V^C + V^I \boldsymbol{I}^2 + V^{T2}\,[T_2, Y_2]_0 + V^{T2'}\,[T'_2, Y_2]_0 + V^{T4}\,[T_4, Y_4]_0 , \qquad (3)$$

where

$$T_{\lambda\mu} = \sum_{i\in\mathrm{Ar}} y_{\lambda\mu}(\boldsymbol{\xi}_i) , \qquad T'_{2\mu} = \sum_{i\in\mathrm{Ar}} \xi_i^2 y_{2\mu}(\boldsymbol{\xi}_i) , \qquad (4)$$

and $\boldsymbol{I}$ is the angular momentum of ^{38}Ar. The nucleon-nucleon interaction adopted is the Hasegawa-Nagata-Yamamoto force [21] with depth parameter $V_0(^3E) = -485$ MeV for the intermediate range. As for the Coulomb interaction, only the central part is adopted, and the tensor parts derived from the Coulomb force are very small and are neglected. The depths V^{T2} and $V^{T2'}$ are multiplied by factors 1.4 and 0.6, respectively, so as to reproduce the low-lying states energies; these factors are similar to those used in the ^{40}Ca system.

A. Energy spectra

The OCM equation is solved for all spin-parity states up to $J = 12$. The calculated and observed energy spectra are shown in Fig. 1, where the energies are given with respect to the $\alpha+^{38}$Ar threshold ($E_{\mathrm{th}} = 6.26$ MeV). In the experimental spectrum, many levels above $E = -2$ MeV which do not have definite spin and parity assignments are omitted. The 0_1^+($E_{\mathrm{x}} = 0.0$ MeV), 2_1^+(1.52 MeV), 4_1^+(2.75 MeV), and 6_1^+(3.13 MeV) states

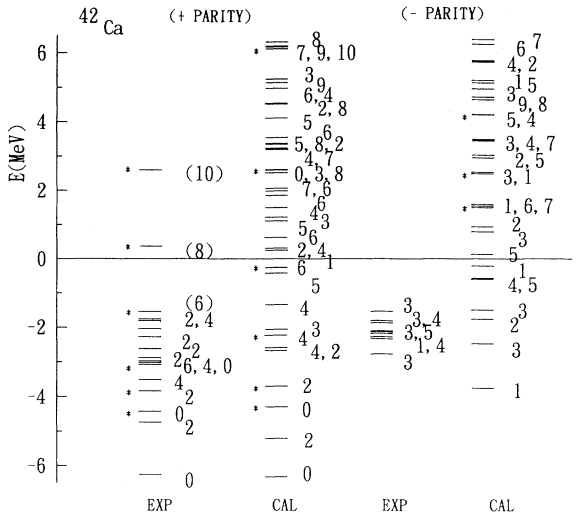

FIG. 1. Calculated and experimental energy spectra of ^{42}Ca. The energy scale is measured from the α threshold. The states marked by an asterisk are the members of $\alpha+^{38}\mathrm{Ar}(0^+)$ cluster bands. Experimental energies are from Ref. [22].

are largely of $2p$ nature. The levels marked by an asterisk are generally assumed to be the $4p$-$2h$ deformed states and form a $K = 0^+$ band [15,20]. The $E2$ transitions of these levels show strong enhancements comparable to those of the α-cluster band in ^{40}Ca. The 0^+ and 2^+ members of the band are populated by the α-transfer reaction [14]. The α-transfer strengths to these states, however, are small compared with those to the ground 0^+ state. This might complicate the argument, but would not alter the main points.

There are 12 positive-parity levels calculated to be below the α threshold. Three of these are the $(fp)^2$ dominant states of $J = 0_1^+, 2_1^+$, and 4_1^+. All the other levels are the α-cluster states. The members of the predominantly $\alpha+^{38}\mathrm{Ar}(0^+)$ cluster band are also marked by an asterisk, and these are in good agreement with the experimental $K{=}0^+$ cluster band. The calculated 8^+ and 10^+ levels are somewhat higher than the experimental ones. The inclusion of components with $[f] = [31]$ symmetry due to the spin-orbit force would be important to improve the agreement.

The remaining $2_3^+, 3_3^+, 4_3^+$, 5_1^+, and 1_1^+ levels are the members of the $\alpha+^{38}\mathrm{Ar}(2^+)$ cluster band. As the excitation energy of the $^{38}\mathrm{Ar}(2^+)$ is 2.17 MeV, it is reasonable that the $\alpha+^{38}\mathrm{Ar}(2^+)$ cluster band starts about 2 MeV above the 0_2^+ state which has the $\alpha+^{38}\mathrm{Ar}(0^+)$ cluster structure. The excitation energy of the experimental 2_3^+(3.39 MeV) state makes it a good candidate for the calculated 2_3^+ state. A further support to this interpretation is provided by the $E2$ transitions from the state as discussed later. As for the other members of the $\alpha+^{38}\mathrm{Ar}(2^+)$ cluster band, it is difficult to identify the experimental counterparts, due to the lack of experimental information. The energy splitting of the weak coupling multiplet $(I \times l) = (2 \times 2)$ is fairly large. In particular, the 0_3^+ state is predicted to be around 2 MeV above the α threshold. This is ascribed to the coupling

with the ground 0^+ state, which pushes up the 0_3^+ state. This is in sharp contrast to the ^{40}Ca case, in which the 0_3^+ state does not couple with the ground 0^+ state. We cannot consider the experimental 0_3^+(3.30 MeV) state as the candidate, because of its occurrence at energy lower than the 2_3^+ state. It is attractive to assign the experimental 0_3^+ state to a possible $8p$-$6h$ state. Also in ^{40}Ca, the 0_3^+(5.21 MeV) is usually classified as a $8p$-$8h$ state [15,13]. The $8p$-nh states may be present systematically in the ^{40}Ca region. To our regret, the $8p$-nh states are outside the framework of the present model. The higher nodal α-cluster band is predicted to start at about 8 MeV above the α threshold in the present calculation. This result is quite similar to the one in the ^{40}Ca nucleus. These nuclei are better suited to confirm experimentally the higher nodal states.

The low-lying negative-parity states are largely $3p$-$1h$ states. If the spin-orbit splittings of single-particle orbits are taken into account, the agreement of ordering of the levels might be improved. The $K = 0^-$ band of the parity-doublet α+^{38}Ar(0^+) cluster band is predicted to start 1.41 MeV above the α threshold. This is a close analogue of the negative-parity α-cluster bands in ^{40}Ca and ^{44}Ti. The calculated $K = 0^-$ band as well as the $K = 0^+$ band are in good agreement with the predictions [23] calculated using a real part of the optical potential which was obtained from an analysis of the backward angle anomaly in α+^{38}Ar scattering [24]. It is important to search for the experimental members of the $K = 0^-$ α-cluster band. The α-transfer reactions such as ^{38}Ar(^{6}Li,d)^{42}Ca would be very suited for this purpose.

B. Wave functions and α-spectroscopic factors

We show the calculated wave functions and α-spectroscopic factors of α+^{38}Ar(0^+) channel in Table II. The calculated states are classified according to their main components. The $2p$ states are dominated by the lowest $N = 10$ components and contain about 13% mixture of higher components. These mixing character of the $2p$ states are analogous to the $2p$ states in ^{18}O [25]. The S_α^2 factors of the $2p$ states are about 0.04, which is rather smaller than that of the ground 0^+ state in ^{40}Ca [13]. The 4_1^+ state is somewhat different from the others and appears to contain appreciable (40%) higher components. The mixing of shell-model states and α-cluster states is peculiarly large in this state. This is because the 4_1^+ state lies close in energy to the 4_2^+ state which is largely α-cluster state in character.

The positive-parity α+^{38}Ar(0^+) cluster states contain few $N = 10$ components and are dominated by the components with higher quanta. Furthermore, these states have large S_α^2 factors, which can be interpreted as indicating a well-developed α-cluster structure. The 4_2^+ state contains rather a large $N = 10$ component; this is ascribed to the coupling with the 4_1^+ of $2p$ state.

It can also be seen that the mixture of the N=11 component in the negative-parity α+^{38}Ar(0^+) cluster band

TABLE II. Squared norm and α-spectroscopic factors of the wave functions of ^{42}Ca.

J^π	E(MeV)		S_α^2	N		
	CAL	EXP	CAL	10	12	14
$2p$ states						
0_1^+	-6.43	-6.26(0.00)	0.042	0.868	0.024	0.088
2_1^+	-5.30	-4.74(1.52)	0.042	0.867	0.031	0.080
4_1^+	-2.69	-3.51(2.75)	0.095	0.580	0.254	0.095
6^+	1.84	-3.07(3.15)	0.008	0.931	0.024	0.032
α+^{38}Ar(0^+) states						
0^+	-4.39	-4.42(1.84)	0.159	0.021	0.658	0.132
2^+	-3.78	-3.84(2.42)	0.148	0.030	0.658	0.131
4^+	-2.30	-3.01(3.25)	0.069	0.331	0.450	0.103
6^+	-0.28	-1.54(4.72)	0.113	0.001	0.702	0.136
8^+	2.62	0.37(6.63)	0.067		0.711	0.141
10^+	6.92	2.59(8.85)	0.046		0.822	0.092
12^+	11.35		0.043		0.878	0.071
				11	13	15
$3p$-$1h$ states						
1_1^-	-3.82	-2.37 (3.89)	0.102	0.725	0.097	0.117
3_1^-	-2.51	-2.81 (3.45)	0.084	0.743	0.096	0.106
5_1^-	-0.58		0.006	0.758	0.087	0.105
7_1^-	1.56		0.004	0.771	0.082	0.100
α+^{38}Ar(0^+) states						
1^-	1.41		0.242	0.071	0.428	0.184
3^-	2.41		0.237	0.062	0.438	0.185
5^-	4.15		0.184	0.049	0.450	0.190
7^-	7.61		0.122	0.043	0.492	0.182
9^-	11.04		0.105	0.199	0.445	0.150
11^-	15.87		0.123	0.001	0.676	0.151

TABLE III. Spectroscopic factors S_α^2 of α+^{38}Ar($I^\pi = 0^+, 2^+, 4^+$) channels for the positive parity states.

J_i^π	channel (Ixl)								
	(0x0)	(2x2)			(4x4)				
0_1^+	0.042	0.094			0.062				
0_2^+	0.159	0.038			0.001				
0_3^+	0.099	0.200			0.043				
		(2x2)			(4x4)				
1_1^+		0.231			0.008				
	(0x2)	(2x0)	(2x2)	(2x4)	(4x2)	(4x4)	(4x6)		
2_1^+	0.042	0.010	0.018	0.056	0.006	0.011	0.050		
2_2^+	0.148	0.015	0.015	0.013	0.001	0.001	0.002		
2_3^+	0.000	0.103	0.086	0.001	0.002	0.001	0.000		
		(2x2)	(2x4)		(4x2)	(4x4)	(4x6)		
3_1^+		0.170	0.017		0.003	0.001	0.000		
	(0x4)	(2x2)	(2x4)	(2x6)	(4x0)	(4x2)	(4x4)	(4x6)	(4x8)
4_1^+	0.095	0.005	0.006	0.029	0.001	0.001	0.002	0.005	0.046
4_2^+	0.069	0.041	0.015	0.027	0.001	0.001	0.001	0.003	0.025
4_3^+	0.003	0.086	0.092	0.000	0.004	0.001	0.000	0.001	0.000
	(0x6)	(2x4)	(2x6)	(2x8)	(4x2)	(4x4)	(4x6)	(4x8)	(4x10)
6_1^+	0.113	0.055	0.005	0.001	0.004	0.001	0.001	0.000	0.000
6_2^+	0.015	0.081	0.072	0.000	0.012	0.000	0.001	0.000	0.000
	(0x8)	(2x6)	(2x8)	(2x10)	(4x4)	(4x6)	(4x8)	(4x10)	(4x12)
8_1^+	0.067	0.087	0.002	0.001	0.016	0.001	0.000	0.000	0.000
8_2^+	0.034	0.043	0.061	0.000	0.021	0.000	0.001	0.000	0.000

is, on the average, larger than the mixture of the N=10 component in the positive-parity cluster band. The coupling between shell-model states and cluster states becomes stronger in the $K = 0^-$ band than in the $K = 0^+$ band. This situation is similar to ^{40}Ca, but is not so conspicuous. Contrary to the ^{40}Ca case, the S_α^2 factors of the $K = 0^-$ band are still larger than the ones of the $K = 0^+$ band.

In order to analyze the channel components of the wave functions, the spectroscopic factors S_α^2 of the α+^{38}Ar($I^\pi = 0^+, 2^+, 4^+$) channels are listed in Tables III and IV. The 0_1^+ and 2_1^+ states possess relatively large values of S_α^2 in all channels. This is ascribed to a nonorthogonality of channel wave functions with low oscillator quanta and is characteristic of shell-model states. States 0_2^+, 2_2^+, 4_2^+, 6_1^+, and 8_1^+ are approximated by a single channel and are mainly α+^{38}Ar(0^+) cluster states. This interpretation is less clear for the 4_2^+ and 8_1^+ states. Both of the 4_1^+ and 4_2^+ states have large S_α^2 values in $(I \times l) = (0 \times 4)$ channel, which is a result of large mixing of the states. The 8_1^+ state is a mixture of (0×8) and (2×6) cluster configurations, which is due to the closeness of the unperturbed energies of these configurations. It can also be seen that the states 0_3^+, 1_1^+, 2_3^+, 3_1^+, 4_3^+, 6_2^+, and 8_2^+ are largely α+^{38}Ar(2^+) cluster states. These results confirm the weak coupling picture of α+^{38}Ar cluster states.

In the negative-parity states, the 1_3^-, 3_4^-, and 5_4^- states have the largest S_α^2 factors in the $(0 \times l)$ channel and are dominantly α+^{38}Ar(0^+) cluster states. Many states be-

TABLE IV. Spectroscopic factors S_α^2 of α+^{38}Ar($I^\pi = 0^+, 2^+, 4^+$) channels for the negative parity states.

J_i^π	channel (Ixl)								
	(0x1)	(2x1)	(2x3)		(4x3)	(4x5)			
1_1^-	0.102	0.013	0.043		0.006	0.004			
1_2^-	0.005	0.122	0.007		0.087	0.009			
1_3^-	0.242	0.050	0.068		0.004	0.002			
	(0x3)	(2x1)	(2x3)	(2x5)	(4x1)	(4x3)	(4x5)	(4x7)	
3_1^-	0.084	0.001	0.003	0.046	0.008	0.005	0.002	0.002	
3_2^-	0.010	0.068	0.001	0.000	0.049	0.004	0.020	0.000	
3_3^-	0.015	0.032	0.067	0.003	0.006	0.024	0.056	0.004	
3_4^-	0.237	0.060	0.021	0.031	0.006	0.003	0.001	0.000	
	(0x5)	(2x3)	(2x5)	(2x7)	(4x1)	(4x3)	(4x5)	(4x7)	(4x9)
5_1^-	0.006	0.051	0.001	0.018	0.037	0.019	0.004	0.001	0.001
5_2^-	0.076	0.031	0.006	0.030	0.004	0.001	0.001	0.010	0.001
5_3^-	0.019	0.013	0.057	0.009	0.001	0.004	0.021	0.053	0.002
5_4^-	0.184	0.128	0.006	0.015	0.019	0.005	0.001	0.000	0.000

TABLE V. Wave functions of the three lowest 0^+ states in terms of the SU(3) scheme.

N	(λ,μ)	0_1^+	0_2^+	0_3^+
10	(6,0)	0.931	0.146	0.181
12	(12,4)	0.089	-0.792	0.246
	(10,2)	-0.098	0.171	0.609
	(8,0)	-0.081	0.036	0.305
14	(14,4)	-0.044	0.353	-0.052
	(12,2)	0.046	-0.082	-0.346
	(10,0)	0.288	0.020	-0.117

low these cluster states are largely $3p$-$1h$ states. Some α-cluster strength is spread over these $3p$-$1h$ states. States 1_1^-, 3_1^-, and 5_2^- have a sizable S_α^2 factor in the $(0\times l)$ channel. While the states 1_2^-, 3_2^-, 3_3^-, 5_1^-, and 5_3^- have a sizable S_α^2 factor in the $(2\times l)$ channel. This shows an interesting selectivity in the mixtures of shell-model states and α-cluster states.

Let us consider the mixing of shell-model states and α-cluster states in some more detail. Tables V and VI list the calculated wave functions of some 0^+ and 1^- states in terms of the SU(3) scheme. The components of quanta higher than N=15 are abbreviated. The ground 0_1^+ state is dominated by the (λ,μ)=(6,0) representation and contains the (10,0) as the largest mixing component. A series of (N,4) representations is a leading component of the 0_2^+ state, which indicates the well-developed α+^{38}Ar(0^+) cluster structure of the state. The mixture of the (6,0) component in the 0_2^+ state is not so large. The leading component of the 0_3^+ state is a series of $(N-2,2)$ and $(N-4,0)$ representations. This means that the 0_3^+ state is largely α+^{38}Ar(2^+) cluster state. The mixture of the (6,0) component in the 0_3^+ state is somewhat larger than the one in the 0_2^+ state. These features are clearly confirmed in Fig. 2, which shows the reduced width amplitudes (RWA's), $y(r)$, for the α+^{38}Ar(0^+) and α+^{38}Ar(2^+) channels. Also these represent intuitively the degrees of surface localizations of α cluster.

The 1_3^- state is dominated by a series of (N,4) representations and corresponds to the α+^{38}Ar(0^+) cluster state. The main configurations of the 1_1^- and 1_2^- states are the (9,2) and (8,1) of $3p$-$1h$ states, respectively. The

TABLE VI. Wave functions of the three lowest 1^- states in terms of the SU(3) scheme.

N	(λ,μ)	1_1^-	1_2^-	1_3^-
11	(9,2)	0.791	0.140	-0.201
	(8,1)	-0.029	0.793	-0.049
	(7,0)	-0.313	0.223	0.168
13	(13,4)	0.136	-0.003	0.637
	(12,3)	-0.013	-0.148	-0.130
	(11,2)	-0.263	-0.029	-0.063
	(10,1)	0.021	-0.259	0.015
	(9,0)	0.093	-0.074	-0.014
15	(15,4)	-0.078	0.026	-0.385
	(14,3)	0.027	0.089	0.179
	(13,2)	0.290	0.041	0.016
	(12,1)	-0.001	0.325	-0.025
	(11,0)	-0.160	0.119	0.050

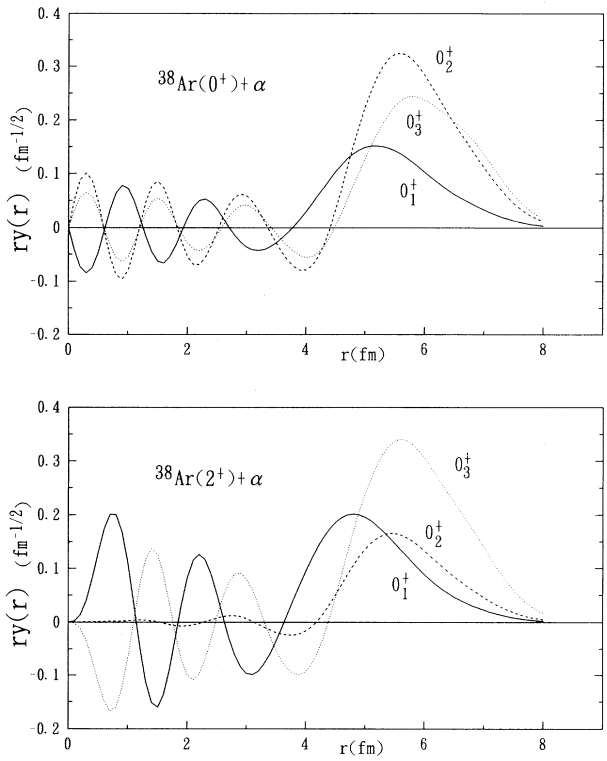

FIG. 2. The reduced width amplitudes of the three lowest 0^+ states for the ^{38}Ar(0^+)+α and ^{38}Ar(2^+)+α channels.

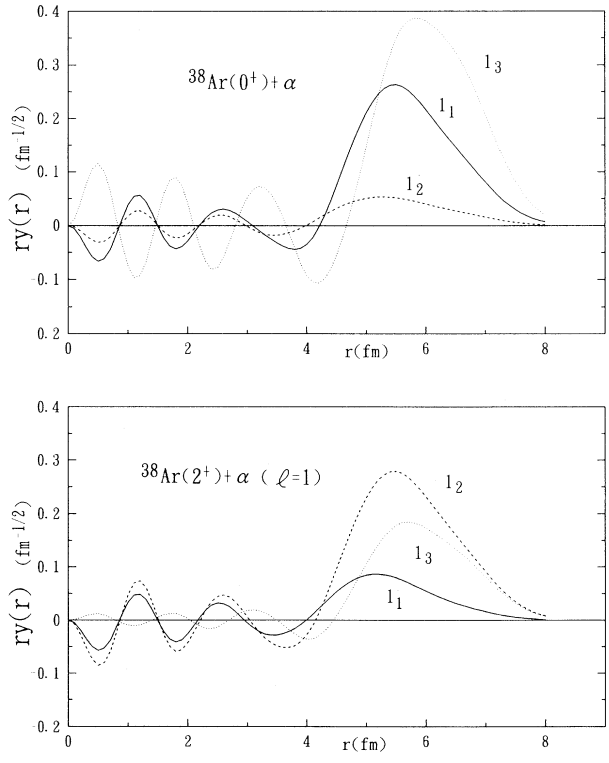

FIG. 3. The reduced width amplitudes of the three lowest 1^- states for the ^{38}Ar(0^+)+α and ^{38}Ar(2^+)+α (l = 1) channels.

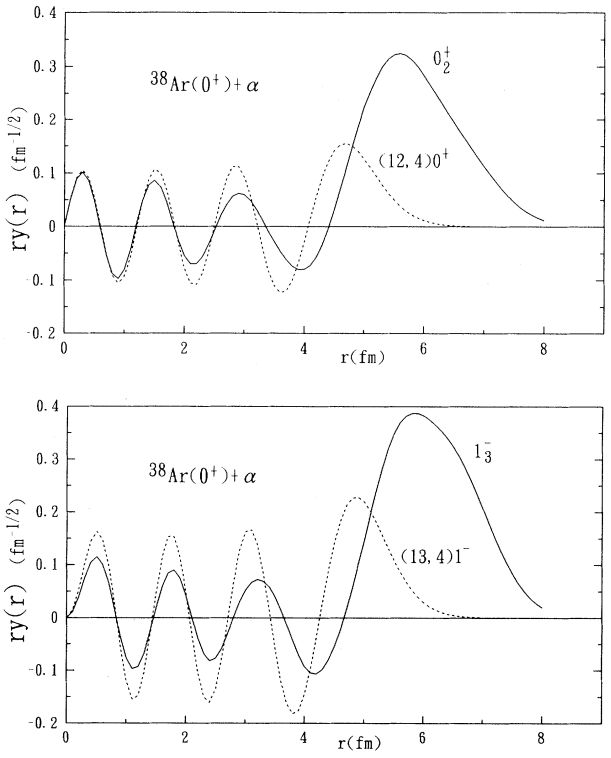

FIG. 4. Comparison of the reduced width amplitudes in the ^{38}Ar(0$^+$)+α channel by the SU(3) shell-model with those by the present cluster model.

(9,2) component of the 1_1^- state leads to strong coupling with a series of (λ, μ=even) representations, which correspond to $\alpha+^{38}$Ar(0$^+$) cluster state, whereas the (8,1) component of the 1_2^- state leads to strong coupling with a series of (λ, μ=odd) components, which can be viewed as the $\alpha+^{38}$Ar(2$^+$) cluster state. The RWA's of the 1$^-$ states for the ^{38}Ar(0$^+$)+$\alpha(l$=1) and ^{38}Ar(2$^+$)+$\alpha(l$=1) channels are shown in Fig. 3, where we can clearly understand the mixing properties of the 1$^-$ states. These features of the mixing of shell-model states and α-cluster states are similar to the ones in ^{40}Ca.

Figure 4 compares the RWA's in the ^{38}Ar(0$^+$)+α channel given by the SU(3) shell model with those of the calculated α-cluster wave functions. The (12,4)$J^\pi = 0^+$ and (13,4)$J^\pi = 1^-$ states are expected to describe the lowest state with 2 and 3 quanta of excitation, respectively. We can clearly see a large difference in the position and height of the outermost peak of the RWA's. It is evident that the shell-model description of the α-cluster states is quite inadequate.

C. Electric transitions and charge form factors

The matrix elements of the electric transitions and charge form factors can be calculated by the method given in Refs. [7,26] using the knowledge of the norm kernel. The reduced matrix elements of the subunit clusters ^{38}Ar and α are taken to be the SU(3) shell-model values.

The calculated value of the root mean square charge radius of the ground state is 3.39 fm, which agrees well with the observed value of 3.46 fm [27]. As for the monopole transition from the 0_2^+(1.84 MeV) to the ground 0$^+$ state, the calculated value is 2.77 fm^2 and only a half of the experimental value of 5.24± 0.39 fm^2 [28]. The transition is affected sensitively by the small mixings of α-cluster and $2p$ configurations of these states. We can only expect the model to give qualitative agreement with such a transition.

In Fig. 5 we present the calculated and experimental $B(E2)$ values. In this calculation, an additional charge $\delta e = 0.3e$ is used, which is smaller than the values of $0.7e \sim 1.0e$ required by the shell-model calculations [32]. Large enhancements of the $\alpha+^{38}$Ar in-band tran-

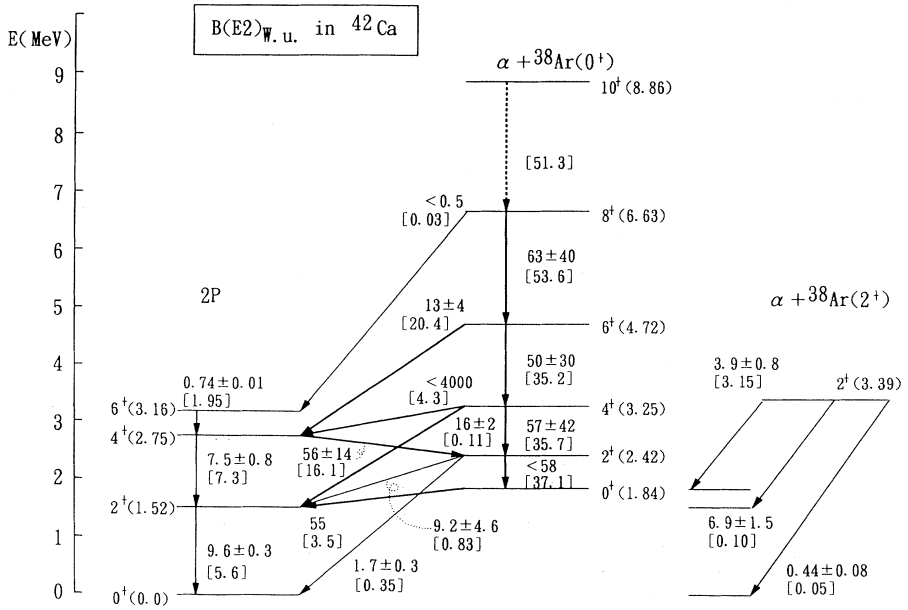

FIG. 5. Calculated and experimental $E2$ transitions of ^{42}Ca. Transitions are in W.u. The numbers are the experimental rates from Refs. [29–31,22], and the numbers in parentheses are the calculated rates. Classification of the spectra into several bands has been done according to their main components.

sitions are reproduced very well, which are almost the same as the α+^{36}Ar in-band transitions in ^{40}Ca. This tends to support the similarities between the α-cluster structures in ^{42}Ca and ^{40}Ca. Agreement with the experiment is achieved also for the transitions of the $2p$ dominant states and for the interband transitions between the α+^{38}Ar and $2p$ states. It is notable that the 2^+(3.39 MeV) $\rightarrow$ 0^+(1.84 MeV) transition is nicely reproduced. This agreement supports our assignment of the 2_3^+ to the α+^{38}Ar(2^+) cluster state. There is a problem about the interband transitions such as the 0_2^+(1.84 MeV) $\rightarrow$ 2_1^+(1.52 MeV) transition. The present model gives a value of 3.5 W.u., which shows some enhancement, but is far smaller than the observed value of 55 W.u. According to Ref. [31], the observed value was determined with an accuracy of less than 2%. The magnitude of the transition is the same order as the in-band transitions of the α-cluster band. It would be difficult to reproduce such a large value as an interband transition between α-cluster and $2p$ states. The interband transitions, however, are very sensitive to mixing properties of the states.

There has been a problem associated with the quadrupole moment of the 2_1^+ state [32,33]. The value calculated by the shell model is positive and small, while the measured value is negative and large. The present calculation gives a negative value of -14.3 e fm^2, which nicely reproduces the experimental value of -19 ± 8 e fm^2 [29]. The 2_1^+ state is admixed somewhat with the α+^{38}Ar cluster states so that the quadrupole moment comes primarily from the cluster components. These electric transitions and quadrupole moment provide strong evidence for the importance of the coexistence and interplay of the α-cluster states and shell-model states in ^{42}Ca.

There have been some electron scattering measurements on ^{42}Ca [34,35]. Electron scattering can provide significant insight into the studies of structure. The calculated longitudinal form factors for the 2^+, 3^-, and 5^- states are compared with the experimental ones in Figs. 6, 7, and 8. In this calculation, we use an effective charge $\delta e = 0.5e$, which is much smaller than the $1.7e$ required

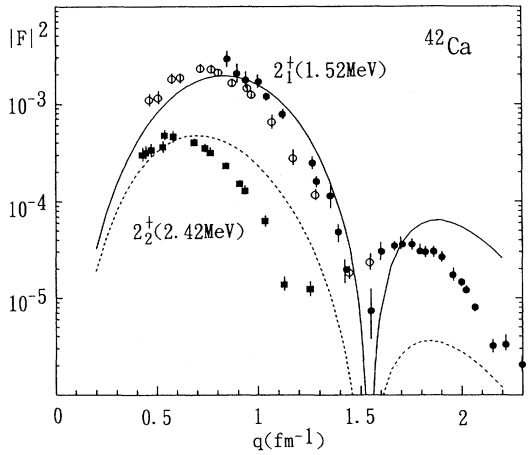

FIG. 6. Calculated and experimental form factors of the 2_1^+ and 2_2^+ states in ^{42}Ca. Experimental data are from Refs. [34,35].

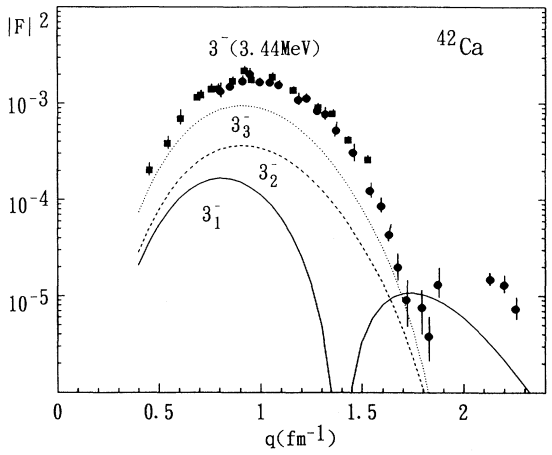

FIG. 7. Calculated and experimental form factors of the 3^- states in ^{42}Ca. Experimental data are from Refs. [34,35].

by the shell-model calculation. An interesting feature is the relative magnitude of the first and second peaks observed in the 2_1^+ form factor, which is difficult to reproduce by the simple $f_{7/2}^2$ shell model [33,35]. The present model gives a good account of these two peaks. The admixture of α-cluster configurations in the 2_1^+ state is responsible for this feature. Furthermore, the 2_2^+ form factor can also be explained by the present model. As pointed out in the previous section, the 2_2^+ is mostly the α+^{38}Ar cluster state. The main properties of the 2_1^+ and 2_2^+ form factors are consistently explained within the present model.

The 3_1^-(3.44 MeV) state has a large transition strength. There are four 3^- levels in the same energy region, which are believed to be mainly $3p$-$1h$ states. The present model predicts three candidates in this energy region. The calculated form factors of the three 3^- levels are compared with the experimental form factor in Fig. 7. All three are not in agreement with the experiment. In order to improve the agreement, it would be important to take into account the configuration mixing due to the spin-orbit splittings of single-particle orbits. The 5_1^-(4.10 MeV) form factor is shown in Fig. 8, which is also mainly a $3p$-$1h$ state. The calculated form factor is somewhat smaller than the experiment.

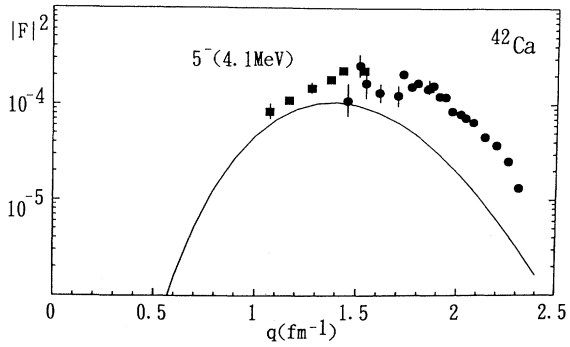

FIG. 8. Calculated and experimental form factors of the 5^- states in ^{42}Ca. Experimental data are from Refs. [34,35].

III. SUMMARY

We have applied the microscopic $\alpha+^{38}$Ar cluster model to ^{42}Ca, in order to attain a unified understanding of its structure. Within this model, the energy spectra, electric transition probabilities, and charge form factors are in very good agreement with the observed values. There remains the problem that a large enhancement of the $0_2^+ \rightarrow 2_1^+$ $E2$ transition is difficult to reproduce by the present model. This, however, may not be so serious, since the interband transition is very sensitive to the mixing properties of the states. The additional charges $0.3e$ and $0.5e$ are required to reproduce the $E2$ transitions and charge form factors, respectively. These are probably ascribed to the core-polarization effects of ^{38}Ar and α. The improvement of this situation is an important area of future work.

It is concluded that the persistency of the α-cluster states in ^{42}Ca is established on a firmer basis. It has been shown that the coexistence and interplay of α-cluster and shell-model structures are essentially responsible for this success. We have also shown an interesting selectivity of the coupling of these two structures. The range of validity of the α-cluster model has thus been extended to non-α nuclei in the fp-shell region.

ACKNOWLEDGMENTS

The authors wish to thank Professor S. Nagata for helpful discussions. We are also grateful to Professor P.E. Hodgson for his careful reading of the manuscript. This work was done as a part of the research projects "Molecule aspects and structure-change in the ^{44}Ti region" organized by the Yukawa Institute for Theoretical Physics, Kyoto University in 1992 and "α-cluster structure and $8p$-nh states in the ^{44}Ti region" organized by the Research Center for Nuclear Physics, Osaka University in 1994. The authors are greatly indebted to the members of the projects.

[1] F. Michel, G. Reidemeister, and S. Ohkubo, Phys. Rev. Lett. **57**, 1215 (1986); Phys. Rev. C **37**, 292 (1988).
[2] S. Ohkubo, Phys. Rev. C **38**, 2377 (1988).
[3] S. Ohkubo and K. Umehara, Prog. Theor. Phys. **80**, 598 (1988).
[4] G. Reidemeister, S. Ohkubo, and F. Michel, Phys. Rev. C **41**, 63 (1990).
[5] K.F. Pal and R.G. Lovas, Phys. Lett. **96B**, 19 (1980).
[6] K. Itonaga, Prog. Theor. Phys. **66**, 2103 (1981).
[7] T. Wada and H. Horiuchi, Phys. Rev. C **38**, 7063 (1988).
[8] A.C. Merchant, Phys. Rev. C **36**, 778 (1987); **37**, 414 (1988); A.C. Merchant, K.F. Pal, and P.E. Hodgson, J. Phys. G **15**, 601 (1989).
[9] T. Yamaya, S. Oh-ami, M. Fujiwara, T. Itahashi, K. Katori, M. Tosaki, S. Kato, S. Hatori, and S. Ohkubo, Phys. Rev. C **42**, 1935 (1990); **41**, 2421(1990).
[10] T. Yamaya, S. Ohkubo, S. Okabe, and M. Fujiwara, Phys. Rev. C **47**, 2389 (1993).
[11] T. Yamaya, M. Saito, M. Fujiwara, T. Itahashi, K. Katori, T. Suehiro, S. Kato, S. Hatori, and S. Ohkubo, Phys. Lett. B **306**, 1 (1993); Nucl. Phys. **A573**, 154 (1994).
[12] C.Y. Kim and T. Udagawa, Phys. Rev. C **46**, 532 (1992); P. Guazzoni, M. Jaskola, L. Zetta, C.Y. Kim, T. Udagawa, and G. Bohlen, Nucl. Phys. **A564**, 452 (1993).
[13] T. Sakuda and S. Ohkubo, Phys. Rev. C **49**, 149 (1994).
[14] H.T. Fortune, R.R. Betts, J.N. Bishop, M.N.I. Al-Jadir, and R. Middleton, Nucl. Phys. **A294**, 208 (1978).
[15] W.J. Gerace and A.M. Green, Nucl. Phys. **A93**, 110 (1967); **A123**, 241 (1969).
[16] B.H. Flowers and L.D. Skouras, Nucl. Phys. **A116**, 529 (1968); **A136**, 353 (1969).
[17] P. Federman and S. Pittel, Phys. Rev. **186**, 1106 (1969).
[18] J.B. McGrory, B.H. Wildenthal, and E.C. Halbert, Phys. Rev. C **2**, 186 (1970).
[19] A.P. Zuker, in *Proceedings of the Topical Conference on the Structure of $1f_{7/2}$ Nuclei, Legnaro, 1971*, edited by R.A. Ricci (Editrice Compositori, Bologna, Italy, 1971), p. 95.
[20] D. Cline, in *Proceedings of the Topical Conference on Physics of Medium Light Nuclei, Firenze, 1977*, edited by P. Blasi and R.A. Ricci (Editrice Compositori, Bologna, Italy, 1978), p. 89.
[21] H. Hasegawa and S. Nagata, Prog. Theor. Phys. **45**,1786(1971); Y. Yamamoto, *ibid.* **52**, 471 (1974).
[22] P.M. Endt, Nucl. Phys. **A521**, 1 (1990); At. Data Nucl. Data Tables **23**, 3 (1979).
[23] S. Ohkubo, in *Book of Abstracts of the 1992 International Nuclear Physics Conference, Wiesbaden, 1992*, edited by U. Grundinger (Wiesbaden, Germany, 1992) p. 1.1.9.
[24] H. Oeschler, H. Schröter, H. Fuchs, L. Baum, G. Gaul, H. Lüdecke, R. Santo, and R. Stock, Phys. Rev. Lett. **28**, 694 (1972).
[25] T. Sakuda, Prog. Theor. Phys. **57**, 855 (1977); T. Sakuda, S. Nagata, and F. Nemoto, Suppl. Prog. Theor. Phys. **65**, 111 (1979).
[26] T. Sakuda, Prog. Theor. Phys. **87**, 1159 (1992).
[27] L. Vermeeren, R.E. Silverans, P. Lievens, A. Klein, R. Neugart, C. Schulz, and F. Buchinger, Phys. Rev. Lett. **68**, 1679 (1992).
[28] H.D. Gräf, H. Feldmeier, P. Manakos, A. Richter, and E. Spamer, Nucl. Phys. **A295**, 319 (1978).
[29] C.W. Towsley, D. Cline, and R.N. Horoshko, Nucl. Phys. **A204**, 574 (1973).
[30] P. Betz, E. Bitterwolf, B. Busshardt, and H. Röpke, Z. Phys. A **276**, 295 (1976).
[31] P.M. Lewis, A.R. Poletti, and M.J. Savage, Nucl. Phys. **A443**, 210 (1985).
[32] J.B. McGrory, Phys. Rev. C **8**, 693 (1973).
[33] T. Iwamoto, H. Horie, and A. Yokoyama, Phys. Rev. C **25**, 658 (1994).
[34] J. Heisenberg, J.S. McCarthy, and I. Sick, Nucl. Phys. **A164**, 353 (1971).
[35] K. Itoh, Y.M. Shin, W.J. Gerace, and Y. Torizuka, Nucl. Phys. **A492**, 426 (1989).